

Supporting Information

Cu(I) diimine complexes as antibacterial photosensitisers operating in water under visible light

Martin V. Appleby,^a Peter G. Walker,^b Dylan Pritchard,^a Sandra van Meurs,^a Carly M. Booth,^a Craig Robertson,^a Michael D. Ward,^c David J. Kelly,^{b*} Julia A. Weinstein^{a*}

^a Department of Chemistry, University of Sheffield, Sheffield S3 7HF, UK

^b Department of Molecular Biology and Biotechnology, University of Sheffield, UK

^c Department of Chemistry, University of Warwick, Coventry CV4 7AL, UK

e-mail: D.Kelly@sheffield.ac.uk, Julia.Weinstein@sheffield.ac.uk

Contents

S1 Synthesis and characterisation	2
S1.1 Estimation of the excited state lifetime needed to achieve a two-fold reduction in the lifetime of a photosensitiser by oxygen.	2
S2 Solid State NMR spectroscopy	4
S3 Crystallographic data for complex 1	8
S3.1 Calculating the volume of the pores in Silica gel used compared to the crystal structure.....	9
S4 Determination of singlet oxygen yield using singlet oxygen probe	28
S5 Bacterial inactivation assay of MRSA in the presence of complex 1 in suspension	31
S6 Stability of 1 -silica.....	31
S6.1 Measuring the amount of leaching of complex 1 from silica through UV-Vis absorption of the suspension in water.....	31
S6.2 Measuring the amount of complex 1 before and after immobilisation on silica. .	32

S7 Summary of relevant photosensitisers used for bacterial killing, as reported to date....34

References 36

S1 Synthesis and characterisation

Scheme S1 Synthesis scheme of complex **1**¹

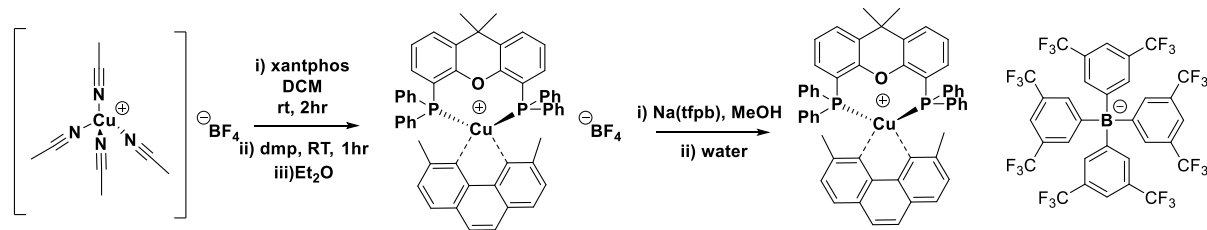


Table S1. Properties of complex **1** in different solvents and in the solid state. a. Uv-vis/absorption maxima; b. molar extinction coefficient measured at the wavelength stated; c. measured at excitation 377 nm, (emission measured at excitation 410 - 415 nm, in DCM under Argon atmosphere); d. lifetime in aerated solution measured using Time Correlated Single Photon Counting (TCSPC); e. lifetime in deaerated solution (under Argon); f. Emission quantum yield in aerated solution. g. singlet oxygen quantum yield.

Solvent	$\lambda_{abs}(\text{nm})^{\text{a}}$	$\epsilon_{abs} \times 10^3$ ($\text{M}^{-1} \text{cm}^{-1}$) ^b	$\lambda_{em}(\text{nm})^{\text{c}}$	$\tau_{\text{O}_2}(\text{ns})^{\text{d}}$	$\tau_{\text{Ar}}(\text{ns})^{\text{e}}$	Φ^{f}	$\phi_{\text{O}_2}(\%)^{\text{g}}$
MeCN	377 (378 ²⁻⁴)	3200 (2800, ^{2,5} 3100 ^{3,4})	568 (552 ⁵ , 564 ³)	62 (64 ³)	220	<0.001	29
MeOH	382	3898	571	93	-	-	-
DCM	384	4290	561 (564 ²)	205	-	-	-
Solid State	374	-	575 (540 ¹)	(5000 ¹)	(30200 ¹)	(0.084 ¹)	-

S1.1 Estimation of the excited state lifetime needed to achieve a two-fold reduction in the lifetime of a photosensitiser by oxygen.

Using the Stern-Volmer equation $\tau_0/\tau = 1 + k\tau_0[\text{O}_2]$, (where τ_0 and τ are excited state lifetimes of PS* without and with the presence of oxygen, respectively), a 0.25 mM oxygen concentration in water under ambient temperature and pressure, and the upper limit of diffusion-controlled reaction k being $1.8 \times 10^{10} \text{ M}^{-1}\text{s}^{-1}$ in water,⁶ one estimates that a 220 ns excited state lifetime without the presence of oxygen would be required to achieve a two-fold reduction in the lifetime of PS* by oxygen, in the reaction potentially leading to ROS.

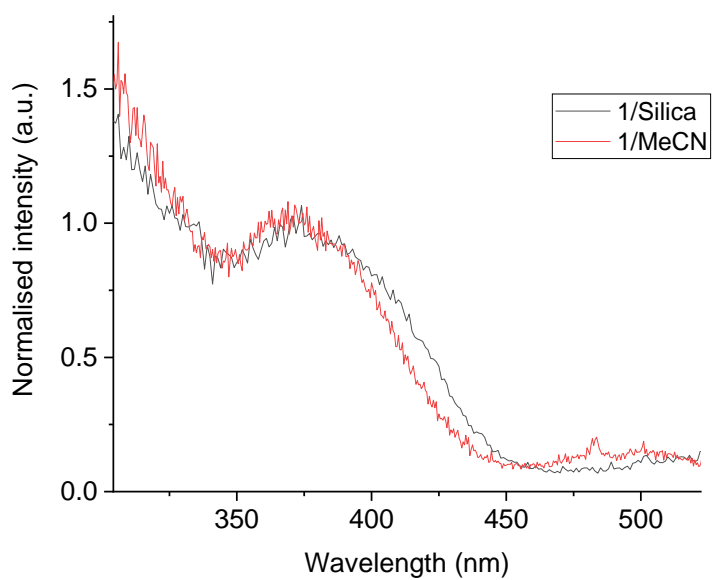


Figure S1. Normalized (to the signal at 373nm) excitation spectra of complex **1** in MeCN solution, and on silica (**1**-silica). Emission detection wavelength was 570 nm.

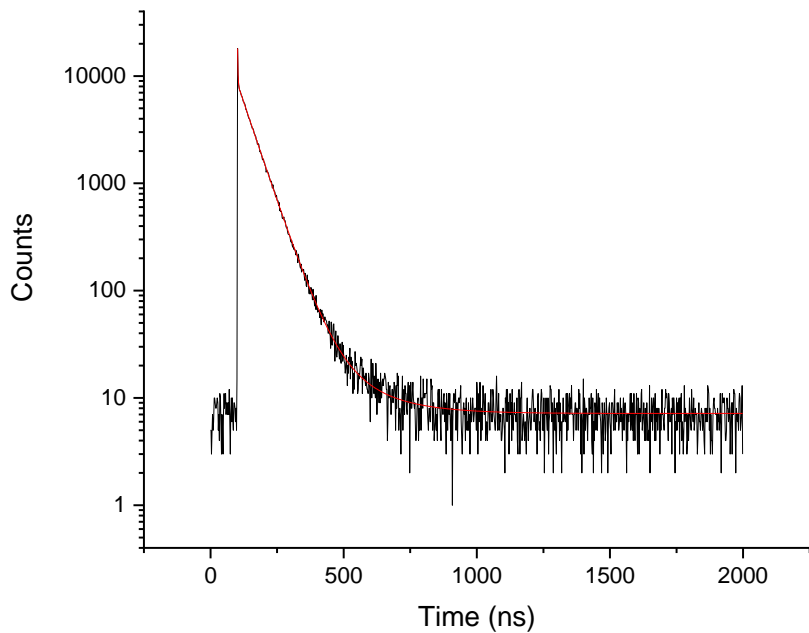


Figure S2. An emission decay trace of complex **1** in aerated MeCN solution (black line), excitation 405 nm (90 ps), registration in the range 525 – 575 nm. A principal decay component is 58 ns. A small contribution at early times is due to the instrument response function.

S2 Solid State NMR spectroscopy

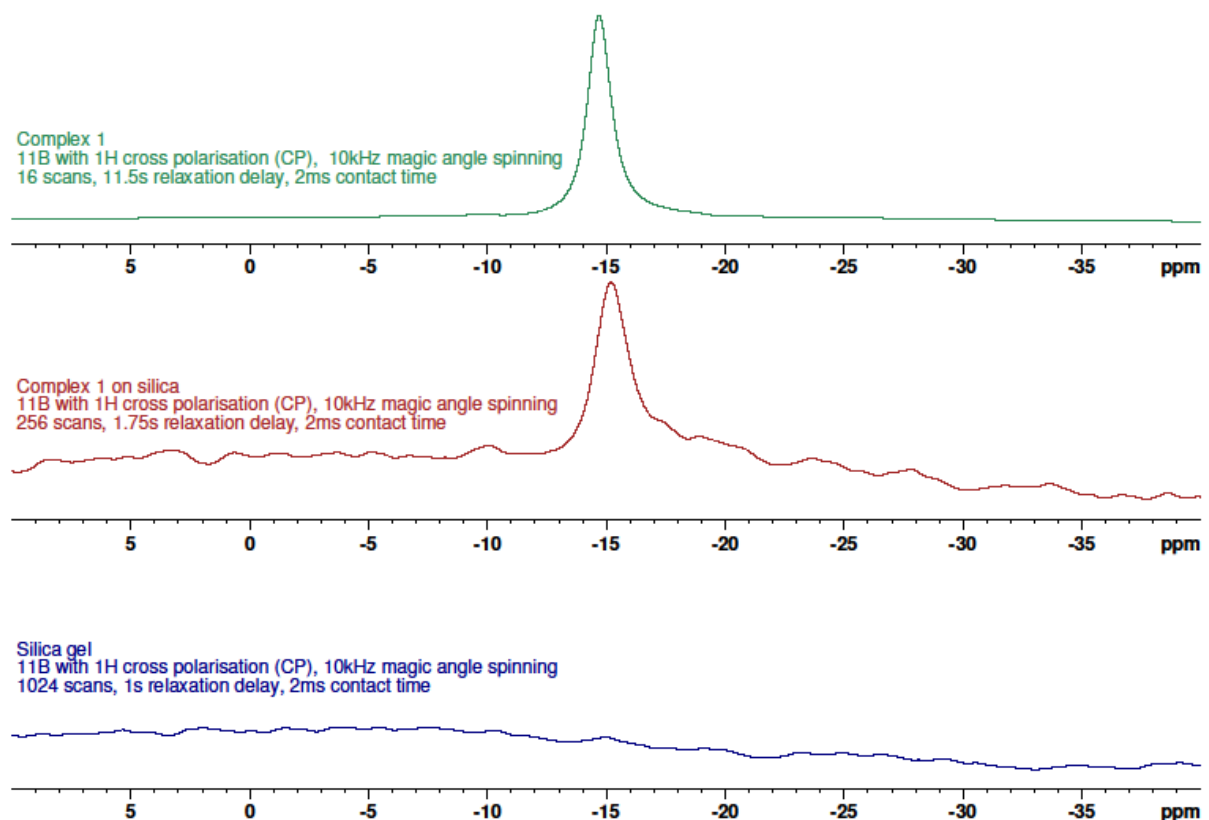


Figure S3. ^{11}B with ^1H cross polarization (CP) solid state NMR of complex **1**, **1** on silica, and silica. The parameters used are stated in the legends

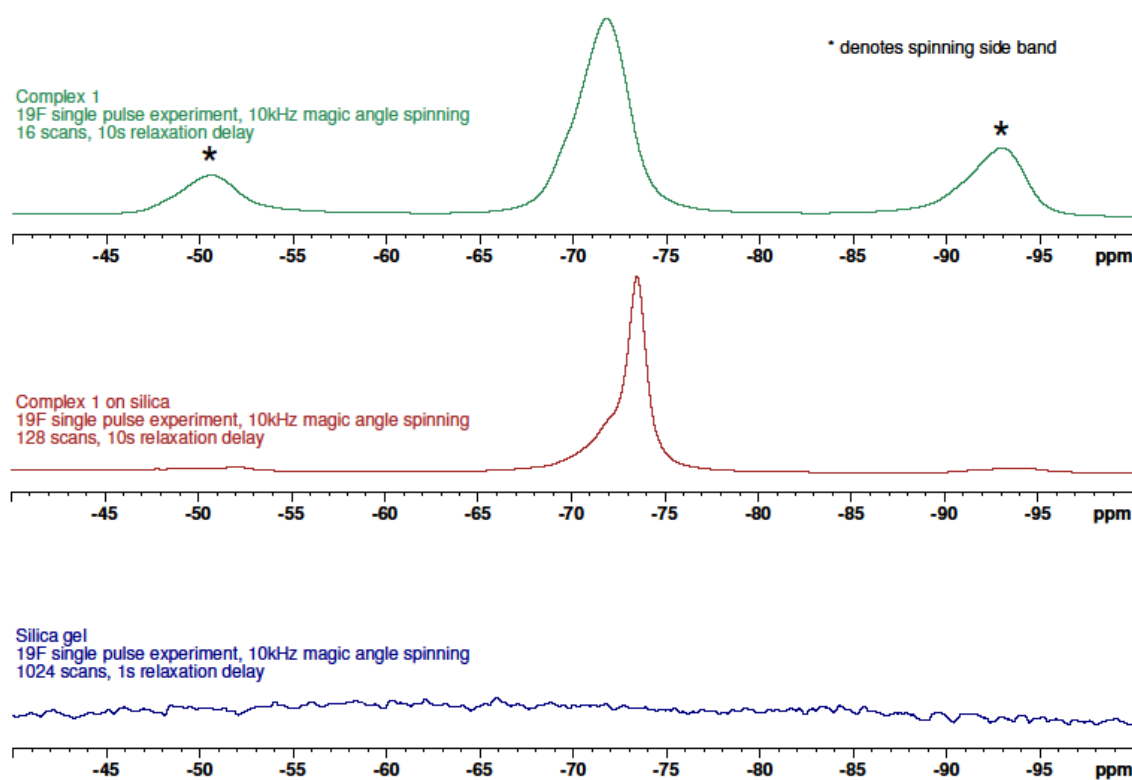


Figure S4. ^{19}F single pulse solid state NMR of complex **1**, complex **1** on silica and silica gel. *denotes spinning side bands.

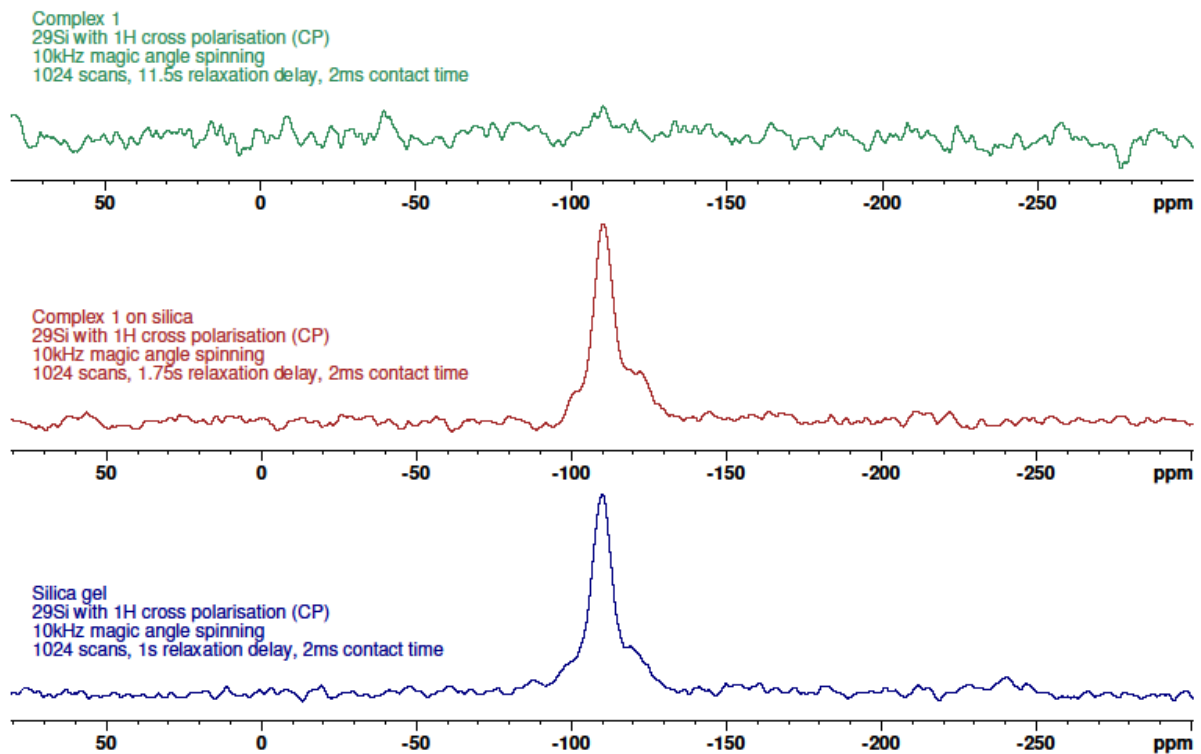


Figure S5. ^{29}Si with ^1H cross polarization (CP) solid state NMR of complex **1** (top), complex **1** on silica (middle) and silica gel (bottom).

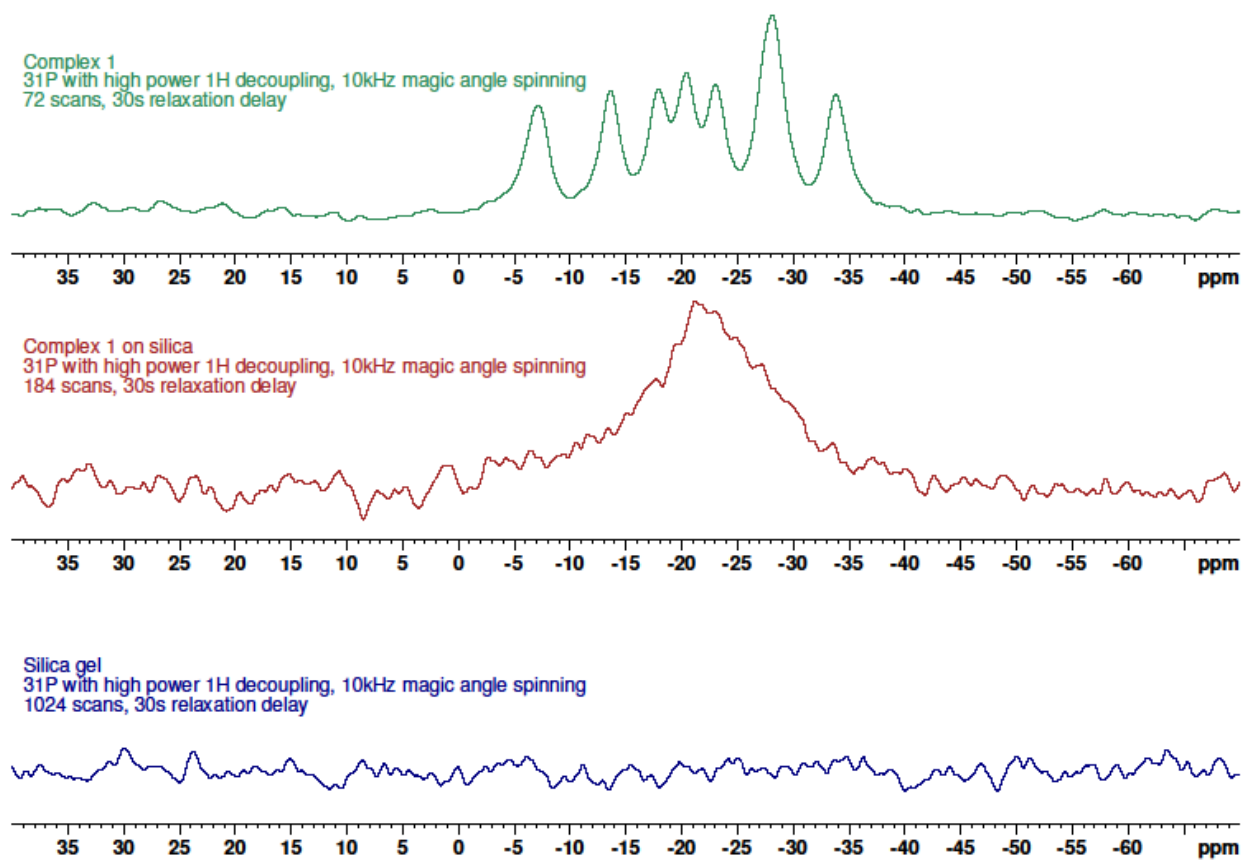


Figure S6. ^{31}P with high power ^1H decoupling solid state NMR of complex **1**, complex **1** on silica and silica gel.

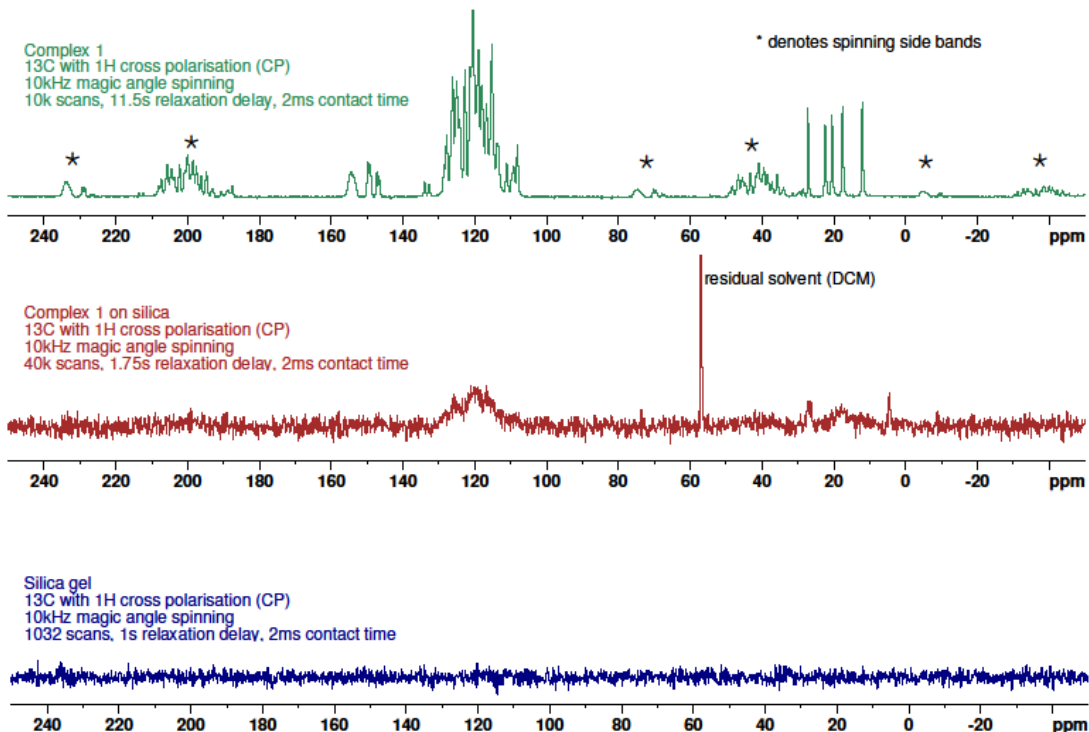


Figure S7. ^{13}C with ^1H cross polarization (CP) solid state NMR of complex **1**, complex **1** on silica and silica gel. *denotes spinning side bands. Residual solvent (DCM) peak from immobilisation method.

S3 Crystallographic data for complex **1**

The results of X-ray crystallographic study of a single crystal of **1** are given in Figure S8.

Intensity data was collected at 100 K on a Bruker D8 Venture diffractometer equipped with a Photon 100 CMOS detector using a CuK α microfocus X-ray source from a crystal mounted in fomblin oil on a MiTiGen microloop and cooled in a stream of cold N₂. Data were corrected for absorption using empirical methods (SADABS⁷) based upon symmetry equivalent reflections combined with measurements at different azimuthal angles⁸. The crystal structures were solved and refined against F2 values using ShelXT⁹ for solution and ShelXL¹⁰ for refinement accessed via the Olex2 program¹¹. Non-hydrogen atoms were refined anisotropically. Hydrogen atoms were placed in calculated positions with idealized geometries and then refined by employing a riding model and isotropic displacement parameters.

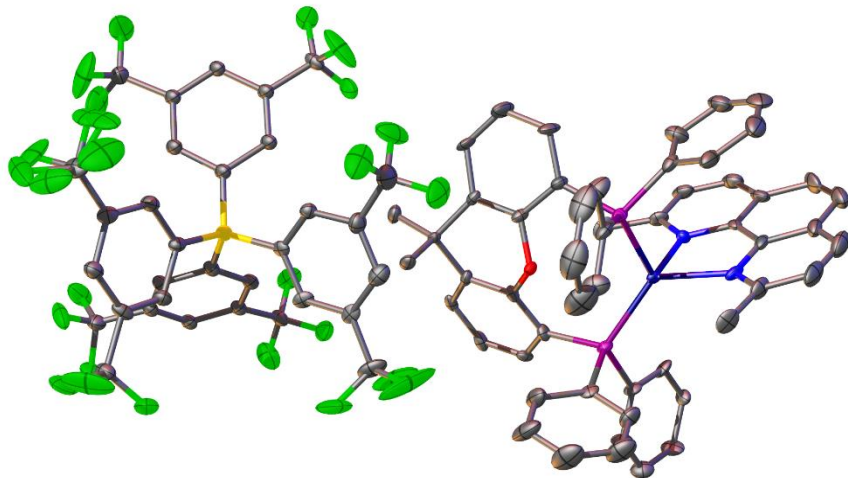


Figure S8. Structure of complex **1** obtained by single crystal X-ray crystallography. Thermal ellipsoids are drawn at 50% probability levels. Hydrogen atoms are omitted for clarity. C (grey), F (green), B (yellow), N (blue), O (red), P (purple). The structure is fully consistent with that published previously, and is given here to estimate the size of the $[\text{Cu}(\text{xanphos})(\text{dmp})]^+$ ion. See Table S2 for details.

S3.1 Calculating the volume of the pores in Silica gel used compared to the crystal structure.

The pore size is listed as 60 Å of the silica gel. Assuming this to be the diameter of the pore, and the pore to be hemispheres, the volume estimated using $\frac{2}{3}\pi r^3$ and $r = 30 \text{ \AA}$ would be $\sim 5.7 \times 10^4 \text{ \AA}^3$. The unit cell of the crystal is $3.9 \times 10^3 \text{ \AA}$ (see Table S2) suggesting that multiple unit cells could fit within a pore of the silica. Therefore, it can be assumed that some of the loaded complex could be within the pores on the silica.

Table S2. Crystal data and structure refinement for complex **1**

Identification code	$[\text{Cu}(\text{xant})(\text{dmp})](\text{tfpb})$
Empirical formula	$\text{C}_{85}\text{H}_{56}\text{BCuF}_{24}\text{N}_2\text{OP}_2$
Formula weight	1713.60
Temperature/K	100
Crystal system	Triclinic
Space group	P-1
a/Å	15.2633(5)
b/Å	16.5133(5)
c/Å	16.9715(5)
$\alpha/^\circ$	102.705(2)
$\beta/^\circ$	108.539(2)

$\gamma/^\circ$	97.064(2)
Volume/ \AA^3	3869.3(2)
Z	2
$\rho_{\text{calc}} \text{g/cm}^3$	1.471
μ/mm^{-1}	1.734
F(000)	1736.0
Crystal size/mm ³	0.1 × 0.05 × 0.015
Radiation	CuK α ($\lambda = 1.54178$)
2 Θ range for data collection/°	5.61 to 134.172
Index ranges	-18 ≤ h ≤ 18, -19 ≤ k ≤ 19, -20 ≤ l ≤ 19
Reflections collected	69044
Independent reflections	13622 [$R_{\text{int}} = 0.2218$, $R_{\text{sigma}} = 0.1289$]
Data/restraints/parameters	13622/1113/993
Goodness-of-fit on F ²	1.115
Final R indexes [$ I >= 2\sigma(I)$]	$R_1 = 0.1417$, $wR_2 = 0.2598$
Final R indexes [all data]	$R_1 = 0.1823$, $wR_2 = 0.2793$
Largest diff. peak/hole / e \AA^{-3}	0.76/-0.74

Table S3. Fractional Atomic Coordinates ($\times 10^4$) and Equivalent Isotropic Displacement Parameters ($\text{\AA}^2 \times 10^3$) for complex **1**. U_{eq} is defined as 1/3 of the trace of the orthogonalised U_{ij} tensor.

Atom X	y	z	U(eq)
Cu1	919.5 (8)	7967.8 (8)	8594.5 (8)
P1	796.2 (16)	6660.0 (14)	8873.7 (14)
P2	2063.4 (15)	8372.4 (14)	8097.7 (14)
O1	1744 (4)	6519 (4)	7665 (4)
N1	554 (5)	8649 (5)	9613 (5)
N2	-449 (5)	8059 (5)	7909 (4)
C1	529 (6)	5738 (5)	7951 (6)

C2	-139 (7)	4982 (6)	7745 (6)	28 (2)
C3	-278 (8)	4329 (7)	7029 (7)	36 (3)
C4	247 (6)	4409 (6)	6510 (6)	24 (2)
C5	949 (6)	5141 (5)	6697 (5)	15.5 (16)
C6	1067 (6)	5779 (5)	7430 (5)	17.3 (17)
C7	1620 (6)	5258 (5)	6212 (6)	15.5 (16)
C8	1723 (6)	6192 (5)	6204 (6)	17.3 (16)
C9	1806 (5)	6498 (6)	5514 (5)	18.0 (17)
C10	1983 (6)	7367 (6)	5615 (6)	22.4 (18)
C11	2094 (6)	7937 (6)	6380 (5)	16.4 (17)
C12	2004 (6)	7675 (6)	7089 (5)	17.5 (17)
C13	1825 (6)	6798 (6)	6962 (5)	16.3 (16)
C14	1248 (6)	4651 (6)	5299 (6)	25 (2)
C15	2579 (6)	5118 (6)	6730 (6)	21.0 (19)
C16	1746 (7)	6423 (6)	9689 (6)	21.3 (13)
C17	2656 (7)	6907 (7)	9950 (7)	35 (2)
C18	3400 (9)	6725 (8)	10546 (8)	55 (3)
C19	3249 (10)	6056 (9)	10894 (8)	55 (3)
C20	2356 (10)	5591 (8)	10649 (8)	51 (3)
C21	1610 (9)	5745 (7)	10046 (7)	38 (3)
C22	-236 (7)	6568 (6)	9188 (6)	21.3 (13)
C23	-1130 (7)	6465 (7)	8563 (7)	32 (2)
C24	-1903 (8)	6580 (7)	8796 (8)	41 (3)
C25	-1789 (9)	6800 (7)	9655 (9)	47 (3)
C26	-945 (9)	6873 (7)	10288 (8)	44 (3)
C27	-143 (8)	6764 (6)	10060 (6)	30 (2)
C28	3265 (6)	8496 (5)	8817 (6)	18.5 (12)
C29	3868 (7)	7945 (7)	8626 (8)	37 (3)
C30	4752 (8)	8028 (7)	9240 (9)	48 (3)

C31	5063 (8)	8620 (8)	10028 (9)	53 (3)
C32	4486 (8)	9167 (7)	10224 (8)	45 (3)
C33	3601 (7)	9079 (6)	9624 (6)	29 (2)
C34	2084 (6)	9381 (5)	7861 (6)	18.5 (12)
C35	2905 (6)	9902 (6)	7901 (6)	24 (2)
C36	2875 (7)	10662 (6)	7669 (7)	30 (2)
C37	2021 (7)	10912 (6)	7382 (7)	29 (2)
C38	1190 (6)	10398 (6)	7328 (6)	20.5 (19)
C39	1232 (7)	9647 (5)	7551 (6)	21.2 (19)
C40	1031 (8)	8880 (6)	10464 (6)	29 (2)
C41	613 (9)	9196 (7)	11063 (7)	39 (2)
C42	-282 (9)	9278 (7)	10791 (7)	43 (3)
C43	-819 (8)	9052 (6)	9909 (7)	31 (2)
C44	-374 (7)	8720 (5)	9336 (6)	19.9 (17)
C45	-1787 (8)	9127 (7)	9570 (8)	42 (2)
C46	-2274 (8)	8867 (7)	8704 (8)	38 (2)
C47	-1846 (6)	8515 (6)	8106 (7)	26.8 (19)
C48	-909 (6)	8436 (5)	8422 (6)	17.4 (16)
C49	-2328 (7)	8220 (6)	7211 (7)	30 (2)
C50	-1890 (6)	7838 (6)	6687 (7)	28 (2)
C51	-947 (6)	7745 (6)	7065 (6)	21.2 (18)
C52	2024 (7)	8766 (6)	10749 (6)	28.0 (15)
C53	-481 (7)	7287 (6)	6511 (6)	28.0 (15)
F1	4817 (6)	6137 (4)	7836 (6)	78 (3)
F2	6002 (6)	5646 (5)	8113 (9)	114 (4)
F3	5459 (8)	6013 (5)	9081 (5)	111 (4)
F4	3075 (6)	4052 (4)	9398 (4)	57 (2)
F5	2198 (5)	3043 (5)	8284 (4)	58 (2)
F6	3466 (6)	2844 (5)	9155 (5)	58 (2)

F7	236 (4)	2500 (4)	5295 (4)	38.3 (15)
F8	446 (5)	1776 (6)	6194 (5)	67 (2)
F9	-388 (4)	1193 (4)	4871 (6)	68 (3)
F10	1204 (5)	-694 (5)	3571 (6)	90 (3)
F11	2658 (7)	-607 (5)	4308 (5)	81 (3)
F12	2279 (6)	-43 (5)	3297 (5)	67 (2)
F13	3373 (4)	5342 (3)	4895 (4)	30.8 (13)
F14	2437 (4)	4458 (4)	3705 (4)	38.6 (15)
F15	3751 (5)	5188 (4)	3764 (5)	47.3 (17)
F16	4668 (4)	2189 (5)	2789 (4)	52.5 (19)
F17	5886 (4)	3181 (4)	3483 (4)	33.3 (14)
F18	5729 (5)	2075 (4)	3919 (5)	47.9 (18)
F19	7640 (4)	3584 (4)	7392 (5)	46.8 (17)
F20	7822 (5)	2545 (5)	6521 (5)	60 (2)
F21	8189 (4)	2580 (6)	7844 (6)	80 (3)
C54	4025 (6)	3374 (6)	6939 (6)	17.3 (16)
C55	4546 (6)	4194 (6)	7212 (6)	20.2 (18)
C56	4628 (6)	4761 (6)	7998 (6)	18.9 (17)
C57	4151 (7)	4520 (6)	8512 (6)	26.5 (19)
C58	3626 (7)	3710 (6)	8248 (6)	24.8 (19)
C59	3587 (6)	3144 (6)	7490 (6)	19.1 (18)
C60	5194 (7)	5617 (6)	8255 (7)	34 (2)
C61	3079 (8)	3409 (7)	8768 (7)	38 (2)
C62	2971 (6)	1982 (6)	5588 (6)	19.8 (8)
C63	2117 (6)	2151 (6)	5671 (6)	19.8 (8)
C64	1270 (6)	1561 (6)	5246 (6)	19.8 (8)
C65	1225 (6)	786 (6)	4683 (6)	19.8 (8)
C66	2041 (6)	632 (6)	4567 (6)	19.8 (8)
C67	2897 (6)	1202 (6)	5007 (6)	19.8 (8)

C68	393 (6)	1747 (6)	5392 (6)	24.0 (18)
C69	2043 (7)	-177 (6)	3965 (7)	31 (2)
C70	4151 (6)	3071 (6)	5318 (6)	19.5 (8)
C71	3747 (6)	3744 (6)	5112 (6)	19.5 (8)
C72	3841 (6)	4053 (6)	4430 (6)	19.5 (8)
C73	4341 (6)	3706 (6)	3934 (6)	19.5 (8)
C74	4732 (6)	3031 (6)	4133 (6)	19.5 (8)
C75	4641 (6)	2724 (6)	4811 (6)	19.5 (8)
C76	3348 (6)	4753 (6)	4193 (6)	20.7 (17)
C77	5250 (7)	2628 (6)	3600 (6)	26.7 (18)
C78	4868 (6)	2200 (6)	6451 (5)	17.1 (17)
C79	5799 (6)	2625 (6)	6679 (6)	20.2 (18)
C80	6564 (6)	2276 (6)	7011 (6)	20.5 (18)
C81	6439 (6)	1468 (6)	7125 (6)	23.3 (19)
C82	5526 (6)	1022 (6)	6900 (6)	21.5 (18)
C83	4750 (6)	1400 (6)	6578 (6)	22.6 (19)
C84	7557 (6)	2749 (6)	7206 (6)	24.6 (18)
C85	5352 (6)	146 (6)	6979 (6)	32 (2)
B1	3990 (7)	2663 (6)	6069 (6)	18.0 (18)
F22A	5280 (13)	-395 (6)	6227 (8)	72 (4)
F23A	6077 (8)	-26 (7)	7543 (10)	66 (4)
F24A	4581 (7)	-106 (8)	7110 (10)	53 (3)
F22B	5870 (20)	-378 (16)	6780 (30)	80 (9)
F23B	5380 (30)	178 (18)	7793 (13)	83 (8)
F24B	4434 (12)	-254 (19)	6620 (20)	53 (3)

Table S4. Anisotropic Displacement Parameters ($\text{\AA}^2 \times 10^3$) for complex **1**. The Anisotropic displacement factor exponent takes the form: $-2\pi^2[h^2a^{*2}U_{11} + 2hka^*b^*U_{12} + \dots]$.

Atom	U_{11}	U_{22}	U_{33}	U_{23}	U_{13}	U_{12}
Cu1	14.5 (6)	12.5 (6)	8.2 (6)	1.4 (5)	2.1 (5)	-0.2 (5)
P1	21.1 (11)	13.4 (11)	15.1 (11)	4.2 (8)	7.0 (9)	1.6 (9)
P2	16.5 (10)	10.4 (11)	15.8 (11)	4.5 (8)	2.4 (9)	1.4 (8)
O1	20 (3)	11 (3)	14 (3)	0 (2)	7 (2)	2 (2)
N1	30 (3)	12 (4)	13 (3)	0 (3)	5 (3)	-4 (3)
N2	12 (3)	18 (4)	15 (3)	2 (3)	5 (2)	0 (3)
C1	21 (4)	13 (4)	18 (4)	1 (3)	5 (3)	-2 (3)
C2	33 (5)	19 (5)	27 (5)	2 (3)	13 (4)	-13 (4)
C3	41 (6)	25 (5)	30 (5)	-7 (4)	14 (5)	-14 (4)
C4	25 (5)	10 (4)	27 (5)	-2 (3)	4 (4)	-5 (3)
C5	15 (4)	11 (4)	16 (4)	1 (3)	0 (3)	3 (3)
C6	21 (4)	12 (4)	16 (4)	3 (3)	4 (3)	-1 (3)
C7	11 (4)	10 (4)	21 (4)	-1 (3)	5 (3)	-1 (3)
C8	17 (4)	15 (4)	17 (4)	-2 (3)	4 (3)	5 (3)
C9	7 (4)	30 (4)	11 (4)	-2 (3)	0 (3)	4 (3)
C10	17 (4)	37 (4)	15 (4)	5 (3)	6 (4)	12 (4)
C11	12 (4)	20 (4)	14 (4)	4 (3)	3 (3)	-4 (3)
C12	19 (4)	23 (4)	14 (4)	5 (3)	9 (3)	7 (3)
C13	15 (4)	21 (4)	17 (4)	7 (3)	8 (3)	9 (3)
C14	23 (5)	19 (5)	28 (5)	-2 (4)	8 (4)	7 (4)
C15	12 (4)	17 (5)	26 (5)	-1 (4)	2 (3)	1 (3)
C16	32 (3)	11 (3)	20 (3)	3 (2)	9 (2)	4 (2)
C17	28 (4)	33 (6)	38 (6)	17 (5)	0 (4)	5 (4)
C18	46 (6)	47 (7)	45 (7)	6 (5)	-15 (5)	8 (5)
C19	67 (6)	56 (8)	34 (7)	13 (5)	-4 (6)	39 (6)
C20	77 (7)	42 (7)	34 (6)	20 (5)	6 (6)	36 (5)
C21	58 (6)	22 (5)	28 (6)	11 (4)	2 (5)	9 (5)
C22	32 (3)	11 (3)	20 (3)	3 (2)	9 (2)	4 (2)

C23	22 (4)	36 (6)	39 (5)	15 (5)	11 (4)	2 (4)
C24	26 (5)	35 (6)	64 (6)	16 (5)	21 (5)	1 (4)
C25	51 (6)	26 (6)	73 (6)	15 (5)	39 (5)	-5 (5)
C26	66 (6)	32 (6)	49 (6)	10 (5)	42 (5)	5 (5)
C27	45 (5)	19 (5)	25 (4)	2 (4)	18 (4)	-4 (4)
C28	24 (3)	9 (3)	23 (3)	9 (2)	7 (2)	1 (2)
C29	22 (4)	23 (5)	55 (6)	0 (5)	6 (4)	8 (4)
C30	31 (5)	18 (5)	70 (7)	3 (5)	-7 (5)	2 (4)
C31	32 (6)	41 (7)	58 (7)	8 (5)	-15 (5)	6 (5)
C32	38 (6)	33 (6)	41 (6)	5 (5)	-11 (4)	1 (4)
C33	32 (5)	23 (5)	21 (4)	0 (3)	1 (4)	2 (4)
C34	24 (3)	9 (3)	23 (3)	9 (2)	7 (2)	1 (2)
C35	20 (4)	21 (5)	32 (5)	14 (4)	7 (4)	0 (3)
C36	32 (5)	27 (5)	31 (6)	15 (4)	9 (4)	1 (4)
C37	32 (4)	20 (5)	42 (6)	22 (4)	14 (4)	2 (4)
C38	22 (4)	14 (4)	31 (5)	10 (4)	12 (4)	9 (3)
C39	32 (4)	8 (4)	19 (5)	3 (3)	3 (4)	5 (3)
C40	45 (5)	24 (5)	14 (4)	-1 (4)	10 (3)	3 (4)
C41	70 (6)	26 (6)	20 (5)	0 (4)	24 (4)	4 (5)
C42	72 (6)	27 (6)	34 (5)	0 (5)	30 (5)	9 (5)
C43	45 (5)	16 (5)	39 (4)	3 (4)	30 (4)	5 (4)
C44	31 (4)	10 (4)	22 (4)	3 (3)	15 (3)	2 (3)
C45	45 (5)	32 (6)	66 (5)	14 (5)	40 (5)	15 (5)
C46	32 (5)	31 (6)	67 (5)	14 (5)	34 (4)	18 (5)
C47	16 (4)	21 (5)	47 (4)	10 (4)	15 (3)	0 (3)
C48	18 (4)	10 (4)	28 (4)	5 (3)	15 (3)	0 (3)
C49	17 (4)	24 (5)	47 (5)	10 (4)	8 (4)	2 (4)
C50	15 (4)	19 (5)	42 (5)	6 (4)	1 (4)	-1 (3)
C51	14 (4)	21 (5)	19 (4)	3 (3)	-4 (3)	-1 (3)

C52	34 (4)	29 (4)	8 (3)	2 (3)	-8 (3)	6 (3)
C53	34 (4)	29 (4)	8 (3)	2 (3)	-8 (3)	6 (3)
F1	69 (5)	26 (4)	105 (6)	36 (4)	-19 (5)	-13 (3)
F2	50 (5)	40 (5)	232 (12)	-1 (6)	62 (6)	-23 (4)
F3	186 (10)	46 (5)	35 (4)	-5 (3)	-2 (5)	-66 (6)
F4	93 (6)	43 (4)	43 (4)	1 (3)	47 (4)	8 (4)
F5	49 (4)	75 (5)	43 (4)	3 (3)	28 (3)	-18 (3)
F6	103 (6)	48 (4)	44 (4)	24 (3)	43 (4)	24 (4)
F7	30 (3)	32 (3)	67 (4)	18 (3)	29 (3)	17 (3)
F8	45 (4)	141 (8)	58 (4)	66 (5)	40 (4)	52 (5)
F9	11 (3)	43 (4)	119 (6)	-21 (4)	15 (3)	-3 (3)
F10	45 (4)	60 (5)	123 (8)	-55 (5)	38 (4)	-23 (4)
F11	112 (7)	52 (5)	63 (5)	0 (4)	7 (5)	60 (5)
F12	109 (7)	52 (5)	52 (4)	-1 (3)	52 (5)	23 (4)
F13	31 (3)	24 (3)	36 (3)	6 (2)	10 (2)	9 (2)
F14	27 (3)	31 (3)	44 (4)	11 (3)	-6 (3)	8 (2)
F15	59 (4)	54 (4)	65 (5)	46 (4)	45 (4)	30 (3)
F16	30 (3)	68 (5)	40 (4)	-19 (3)	16 (3)	-7 (3)
F17	32 (3)	33 (3)	44 (4)	14 (3)	26 (3)	2 (2)
F18	56 (4)	41 (4)	86 (5)	38 (4)	56 (4)	33 (3)
F19	29 (3)	29 (3)	73 (5)	-3 (3)	23 (3)	-8 (3)
F20	46 (4)	61 (5)	71 (5)	-10 (4)	46 (4)	-17 (3)
F21	17 (3)	111 (7)	97 (6)	76 (6)	-19 (3)	-12 (4)
C54	9 (4)	19 (4)	23 (4)	9 (3)	2 (3)	6 (3)
C55	14 (4)	21 (4)	18 (4)	7 (3)	-6 (3)	2 (3)
C56	16 (4)	19 (4)	18 (4)	8 (3)	-4 (3)	9 (3)
C57	28 (5)	23 (4)	22 (5)	7 (3)	0 (4)	8 (3)
C58	25 (5)	25 (4)	21 (4)	1 (3)	6 (4)	6 (3)
C59	16 (4)	18 (4)	20 (4)	3 (3)	5 (3)	2 (3)

C60	26 (5)	23 (5)	32 (5)	7 (4)	-14 (4)	-5 (4)
C61	47 (5)	37 (6)	33 (5)	2 (4)	23 (4)	7 (4)
C62	13.8 (16)	18.2 (19)	27 (2)	6.1 (15)	5.7 (14)	3.9 (14)
C63	13.8 (16)	18.2 (19)	27 (2)	6.1 (15)	5.7 (14)	3.9 (14)
C64	13.8 (16)	18.2 (19)	27 (2)	6.1 (15)	5.7 (14)	3.9 (14)
C65	13.8 (16)	18.2 (19)	27 (2)	6.1 (15)	5.7 (14)	3.9 (14)
C66	13.8 (16)	18.2 (19)	27 (2)	6.1 (15)	5.7 (14)	3.9 (14)
C67	13.8 (16)	18.2 (19)	27 (2)	6.1 (15)	5.7 (14)	3.9 (14)
C68	16 (4)	31 (5)	34 (5)	18 (4)	12 (3)	10 (3)
C69	25 (4)	24 (5)	40 (5)	-2 (4)	13 (4)	1 (3)
C70	12.5 (16)	22 (2)	22.9 (19)	5.9 (15)	4.5 (14)	3.8 (14)
C71	12.5 (16)	22 (2)	22.9 (19)	5.9 (15)	4.5 (14)	3.8 (14)
C72	12.5 (16)	22 (2)	22.9 (19)	5.9 (15)	4.5 (14)	3.8 (14)
C73	12.5 (16)	22 (2)	22.9 (19)	5.9 (15)	4.5 (14)	3.8 (14)
C74	12.5 (16)	22 (2)	22.9 (19)	5.9 (15)	4.5 (14)	3.8 (14)
C75	12.5 (16)	22 (2)	22.9 (19)	5.9 (15)	4.5 (14)	3.8 (14)
C76	15 (4)	25 (5)	27 (4)	14 (3)	9 (3)	9 (3)
C77	25 (4)	25 (5)	31 (4)	5 (3)	15 (3)	0 (3)
C78	18 (4)	17 (4)	16 (4)	5 (3)	6 (3)	1 (3)
C79	14 (3)	22 (5)	22 (5)	5 (4)	4 (3)	1 (3)
C80	12 (3)	34 (5)	14 (4)	9 (4)	3 (3)	1 (3)
C81	18 (4)	26 (4)	24 (5)	5 (4)	8 (4)	2 (3)
C82	24 (4)	21 (4)	19 (5)	9 (3)	6 (4)	3 (3)
C83	18 (4)	21 (4)	32 (5)	10 (4)	11 (4)	4 (3)
C84	18 (4)	26 (4)	34 (5)	13 (4)	10 (4)	4 (3)
C85	28 (4)	26 (5)	46 (5)	22 (4)	9 (4)	9 (3)
B1	17 (4)	18 (5)	19 (5)	5 (3)	6 (4)	3 (3)
F22A	140 (13)	15 (5)	68 (7)	15 (5)	47 (7)	9 (6)
F23A	42 (5)	42 (7)	96 (9)	44 (7)	-14 (6)	1 (5)

F24A	43 (4)	40 (6)	98 (10)	51 (8)	34 (5)	8 (4)
F22B	85 (16)	50 (14)	180 (30)	80 (18)	102 (19)	49 (14)
F23B	130 (20)	66 (17)	61 (9)	38 (11)	37 (9)	-4 (15)
F24B	43 (4)	40 (6)	98 (10)	51 (8)	34 (5)	8 (4)

Table S5. Bond Lengths for complex 1.

Atom	Atom	Length/Å	Atom	Atom	Length/Å
Cu1	P1	2.309 (3)	C49	C50	1.368 (14)
Cu1	P2	2.259 (3)	C50	C51	1.420 (12)
Cu1	N1	2.116 (8)	C51	C53	1.486 (13)
Cu1	N2	2.086 (7)	F1	C60	1.305 (12)
P1	C1	1.824 (9)	F2	C60	1.327 (14)
P1	C16	1.809 (10)	F3	C60	1.314 (13)
P1	C22	1.816 (10)	F4	C61	1.332 (12)
P2	C12	1.809 (9)	F5	C61	1.314 (13)
P2	C28	1.809 (9)	F6	C61	1.346 (14)
P2	C34	1.796 (9)	F7	C68	1.329 (11)
O1	C6	1.391 (10)	F8	C68	1.328 (11)
O1	C13	1.404 (10)	F9	C68	1.321 (11)
N1	C40	1.334 (12)	F10	C69	1.324 (12)
N1	C44	1.372 (12)	F11	C69	1.312 (13)
N2	C48	1.378 (11)	F12	C69	1.348 (13)
N2	C51	1.336 (11)	F13	C76	1.349 (11)
C1	C2	1.410 (12)	F14	C76	1.334 (10)
C1	C6	1.392 (12)	F15	C76	1.353 (10)
C2	C3	1.375 (14)	F16	C77	1.354 (11)
C3	C4	1.382 (14)	F17	C77	1.342 (11)
C4	C5	1.417 (12)	F18	C77	1.339 (12)

C5	C6	1.388 (12)	F19	C84	1.325 (11)
C5	C7	1.522 (12)	F20	C84	1.339 (11)
C7	C8	1.534 (12)	F21	C84	1.310 (11)
C7	C14	1.532 (12)	C54	C55	1.380 (12)
C7	C15	1.524 (11)	C54	C59	1.399 (12)
C8	C9	1.408 (13)	C54	B1	1.652 (13)
C8	C13	1.397 (12)	C55	C56	1.410 (13)
C9	C10	1.389 (13)	C56	C57	1.390 (14)
C10	C11	1.371 (12)	C56	C60	1.458 (13)
C11	C12	1.405 (12)	C57	C58	1.370 (13)
C12	C13	1.395 (12)	C58	C59	1.393 (13)
C16	C17	1.394 (14)	C58	C61	1.510 (14)
C16	C21	1.407 (14)	C62	C63	1.409 (12)
C17	C18	1.375 (15)	C62	C67	1.408 (12)
C18	C19	1.391 (19)	C62	B1	1.646 (12)
C19	C20	1.366 (19)	C63	C64	1.388 (12)
C20	C21	1.362 (15)	C64	C65	1.398 (12)
C22	C23	1.401 (13)	C64	C68	1.492 (12)
C22	C27	1.400 (13)	C65	C66	1.366 (12)
C23	C24	1.379 (14)	C66	C67	1.385 (12)
C24	C25	1.369 (17)	C66	C69	1.494 (13)
C25	C26	1.362 (18)	C70	C71	1.391 (12)
C26	C27	1.415 (15)	C70	C75	1.388 (12)
C28	C29	1.431 (13)	C70	B1	1.636 (13)
C28	C33	1.385 (13)	C71	C72	1.404 (13)
C29	C30	1.386 (15)	C72	C73	1.386 (12)
C30	C31	1.370 (17)	C72	C76	1.514 (12)
C31	C32	1.397 (17)	C73	C74	1.383 (13)
C32	C33	1.376 (14)	C74	C75	1.394 (13)

C34	C35		1.403 (12)	C74	C77		1.485 (13)
C34	C39		1.402 (12)	C78	C79		1.395 (12)
C35	C36		1.398 (13)	C78	C83		1.384 (12)
C36	C37		1.386 (14)	C78	B1		1.650 (13)
C37	C38		1.402 (13)	C79	C80		1.380 (12)
C38	C39		1.378 (12)	C80	C81		1.389 (13)
C40	C41		1.405 (14)	C80	C84		1.514 (12)
C40	C52		1.486 (14)	C81	C82		1.385 (12)
C41	C42		1.330 (17)	C82	C83		1.417 (13)
C42	C43		1.397 (16)	C82	C85		1.483 (13)
C43	C44		1.411 (13)	C85	F22A		1.351 (11)
C43	C45		1.436 (16)	C85	F23A		1.320 (10)
C44	C48		1.439 (13)	C85	F24A		1.302 (11)
C45	C46		1.359 (17)	C85	F22B		1.303 (14)
C46	C47		1.431 (14)	C85	F23B		1.357 (15)
C47	C48		1.392 (12)	C85	F24B		1.350 (15)
C47	C49		1.400 (15)				

Table S6. Bond Angles for complex **1**.

Atom	Atom	Atom	Angle/ [°]	Atom	Atom	Atom	Angle/ [°]
P2	Cu1	P1	118.33 (9)	C50	C51	C53	119.7 (8)
N1	Cu1	P1	98.7 (2)	C55	C54	C59	115.9 (8)
N1	Cu1	P2	129.4 (2)	C55	C54	B1	123.3 (8)
N2	Cu1	P1	106.4 (2)	C59	C54	B1	120.6 (8)
N2	Cu1	P2	117.1 (2)	C54	C55	C56	121.8 (9)
N2	Cu1	N1	79.6 (3)	C55	C56	C60	119.3 (9)
C1	P1	Cu1	116.2 (3)	C57	C56	C55	120.7 (9)
C16	P1	Cu1	121.3 (3)	C57	C56	C60	120.0 (9)

C16	P1	C1	101.9 (4)	C58	C57	C56	118.3 (9)
C16	P1	C22	107.6 (4)	C57	C58	C59	120.4 (9)
C22	P1	Cu1	103.7 (3)	C57	C58	C61	121.1 (9)
C22	P1	C1	104.9 (4)	C59	C58	C61	118.5 (9)
C12	P2	Cu1	115.1 (3)	C58	C59	C54	122.9 (9)
C28	P2	Cu1	115.9 (3)	F1	C60	F2	101.2 (10)
C28	P2	C12	104.3 (4)	F1	C60	F3	106.3 (10)
C34	P2	Cu1	115.5 (3)	F1	C60	C56	115.8 (8)
C34	P2	C12	102.0 (4)	F2	C60	C56	113.6 (9)
C34	P2	C28	102.0 (4)	F3	C60	F2	103.5 (10)
C6	O1	C13	114.0 (6)	F3	C60	C56	114.8 (10)
C40	N1	Cu1	129.5 (7)	F4	C61	F6	106.2 (9)
C40	N1	C44	117.6 (8)	F4	C61	C58	111.2 (9)
C44	N1	Cu1	111.8 (5)	F5	C61	F4	108.2 (10)
C48	N2	Cu1	114.0 (6)	F5	C61	F6	107.2 (10)
C51	N2	Cu1	128.7 (6)	F5	C61	C58	112.0 (9)
C51	N2	C48	117.1 (7)	F6	C61	C58	111.7 (9)
C2	C1	P1	126.0 (7)	C63	C62	B1	123.8 (8)
C6	C1	P1	116.3 (6)	C67	C62	C63	115.5 (8)
C6	C1	C2	117.6 (8)	C67	C62	B1	120.5 (8)
C3	C2	C1	120.6 (9)	C64	C63	C62	121.9 (8)
C2	C3	C4	119.8 (9)	C63	C64	C65	120.9 (8)
C3	C4	C5	122.3 (9)	C63	C64	C68	120.0 (8)
C4	C5	C7	126.2 (8)	C65	C64	C68	119.0 (8)
C6	C5	C4	115.6 (8)	C66	C65	C64	117.6 (8)
C6	C5	C7	118.1 (7)	C65	C66	C67	122.2 (9)
O1	C6	C1	116.6 (7)	C65	C66	C69	120.6 (8)
C5	C6	O1	119.4 (8)	C67	C66	C69	117.2 (8)
C5	C6	C1	124.0 (8)	C66	C67	C62	121.7 (8)

C5	C7	C8	104.8(7)	F7	C68	C64	112.8(7)
C5	C7	C14	112.2(7)	F8	C68	F7	105.0(8)
C5	C7	C15	108.7(7)	F8	C68	C64	111.5(8)
C14	C7	C8	112.1(7)	F9	C68	F7	105.6(8)
C15	C7	C8	108.6(7)	F9	C68	F8	106.7(9)
C15	C7	C14	110.1(7)	F9	C68	C64	114.5(8)
C9	C8	C7	125.1(8)	F10	C69	F12	102.5(9)
C13	C8	C7	118.0(8)	F10	C69	C66	114.0(8)
C13	C8	C9	116.7(8)	F11	C69	F10	108.7(10)
C10	C9	C8	119.6(8)	F11	C69	F12	103.3(9)
C11	C10	C9	121.4(9)	F11	C69	C66	115.0(9)
C10	C11	C12	122.1(9)	F12	C69	C66	112.1(9)
C11	C12	P2	125.4(7)	C71	C70	B1	121.8(8)
C13	C12	P2	119.7(6)	C75	C70	C71	116.6(9)
C13	C12	C11	114.8(8)	C75	C70	B1	121.5(8)
C8	C13	O1	118.5(8)	C70	C71	C72	121.2(8)
C12	C13	O1	116.0(7)	C71	C72	C76	119.8(8)
C12	C13	C8	125.5(8)	C73	C72	C71	121.6(8)
C17	C16	P1	118.8(7)	C73	C72	C76	118.5(8)
C17	C16	C21	118.6(9)	C74	C73	C72	117.0(9)
C21	C16	P1	122.5(8)	C73	C74	C75	121.4(8)
C18	C17	C16	120.4(11)	C73	C74	C77	118.5(9)
C17	C18	C19	120.1(12)	C75	C74	C77	120.0(8)
C20	C19	C18	119.5(11)	C70	C75	C74	122.1(9)
C21	C20	C19	121.5(12)	F13	C76	F15	105.3(8)
C20	C21	C16	119.9(12)	F13	C76	C72	112.3(8)
C23	C22	P1	119.1(7)	F14	C76	F13	106.3(7)
C27	C22	P1	121.1(7)	F14	C76	F15	107.8(8)
C27	C22	C23	118.6(9)	F14	C76	C72	112.1(7)

C24	C23	C22	121.1(11)	F15	C76	C72	112.7(7)
C25	C24	C23	119.2(11)	F16	C77	C74	112.4(8)
C26	C25	C24	122.1(12)	F17	C77	F16	104.4(8)
C25	C26	C27	119.3(11)	F17	C77	C74	114.1(8)
C22	C27	C26	119.5(10)	F18	C77	F16	105.5(8)
C29	C28	P2	122.2(7)	F18	C77	F17	105.3(8)
C33	C28	P2	120.2(7)	F18	C77	C74	114.3(8)
C33	C28	C29	117.2(9)	C79	C78	B1	119.8(8)
C30	C29	C28	119.1(10)	C83	C78	C79	116.2(8)
C31	C30	C29	121.9(11)	C83	C78	B1	124.1(8)
C30	C31	C32	119.8(10)	C80	C79	C78	122.5(9)
C33	C32	C31	118.7(11)	C79	C80	C81	121.0(8)
C32	C33	C28	123.2(10)	C79	C80	C84	120.2(9)
C35	C34	P2	123.6(7)	C81	C80	C84	118.7(8)
C39	C34	P2	119.4(7)	C82	C81	C80	118.2(9)
C39	C34	C35	116.8(8)	C81	C82	C83	119.9(9)
C36	C35	C34	121.3(9)	C81	C82	C85	120.4(8)
C37	C36	C35	120.1(9)	C83	C82	C85	119.7(8)
C36	C37	C38	119.5(9)	C78	C83	C82	122.1(8)
C39	C38	C37	119.5(9)	F19	C84	F20	105.1(8)
C38	C39	C34	122.6(9)	F19	C84	C80	113.1(8)
N1	C40	C41	121.9(10)	F20	C84	C80	111.1(8)
N1	C40	C52	116.6(9)	F21	C84	F19	107.7(9)
C41	C40	C52	121.4(9)	F21	C84	F20	106.4(9)
C42	C41	C40	120.3(11)	F21	C84	C80	112.9(8)
C41	C42	C43	120.6(10)	F22A	C85	C82	108.0(9)
C42	C43	C44	116.8(10)	F23A	C85	C82	113.4(9)
C42	C43	C45	123.7(10)	F23A	C85	F22A	102.4(11)
C44	C43	C45	119.5(10)	F24A	C85	C82	116.8(9)

N1	C44	C43	122.6(9)	F24A	C85	F22A	105.2(11)
N1	C44	C48	118.2(8)	F24A	C85	F23A	109.6(11)
C43	C44	C48	119.2(9)	F22B	C85	C82	119.9(13)
C46	C45	C43	120.3(10)	F22B	C85	F23B	108(2)
C45	C46	C47	121.5(10)	F22B	C85	F24B	109(2)
C48	C47	C46	119.0(10)	F23B	C85	C82	109.1(14)
C48	C47	C49	117.5(9)	F24B	C85	C82	113.8(15)
C49	C47	C46	123.5(9)	F24B	C85	F23B	92.8(19)
N2	C48	C44	115.8(8)	C62	B1	C54	112.9(7)
N2	C48	C47	123.7(9)	C62	B1	C78	112.1(7)
C47	C48	C44	120.5(8)	C70	B1	C54	114.1(8)
C50	C49	C47	120.0(9)	C70	B1	C62	105.0(7)
C49	C50	C51	119.0(10)	C70	B1	C78	109.9(7)
N2	C51	C50	122.5(9)	C78	B1	C54	103.1(7)
N2	C51	C53	117.7(8)				

Table S7. Hydrogen Atom Coordinates ($\text{\AA} \times 10^4$) and Isotropic Displacement Parameters ($\text{\AA}^2 \times 10^3$) for complex **1**.

Atom X	y	z	U(eq)	
H2	-496.84	4923.86	8104.21	34
H3	-733.06	3822.98	6891.09	43
H4	132.57	3957.55	6009.32	29
H9	1741.34	6113.32	4982.98	22
H10	2028.65	7571.49	5145.29	27
H11	2236.29	8526.71	6431.05	20
H14A	634.45	4750.42	4969.61	37
H14B	1174.78	4063.66	5333.08	37
H14C	1696.12	4752.16	5008.47	37

H15A	3011.98	5174.45	6415.05	32
H15B	2506.19	4548.22	6812.27	32
H15C	2836.97	5542.2	7294.19	32
H17	2761.86	7365.32	9715.03	42
H18	4018.27	7057.77	10720.81	66
H19	3764.12	5923.65	11298.76	66
H20	2251.46	5148.79	10906.18	61
H21	999.88	5396.83	9865.64	46
H23	-1206.58	6313.76	7967.99	38
H24	-2506.49	6507.98	8366.88	49
H25	-2316.61	6904.32	9813.46	56
H26	-893.91	6995.9	10876.4	53
H27	453.14	6822.58	10495.31	36
H29	3665.76	7527.35	8084.97	44
H30	5152.76	7664.2	9110.35	57
H31	5669.23	8658.92	10439.04	63
H32	4700.43	9591.71	10761.48	54
H33	3201.23	9436.43	9770.79	34
H35	3492.85	9733.9	8089.62	29
H36	3440.66	11008.42	7708.33	36
H37	2000.02	11428.46	7223.66	35
H38	602.55	10566.12	7138.07	25
H39	661.32	9294.33	7492.55	25
H41	971.29	9352.04	11664.25	46
H42	-558.34	9491.83	11201.55	52
H45	-2087.69	9358.33	9952.67	50
H46	-2913.65	8921.18	8489.74	46
H49	-2958.94	8285.62	6968.19	36
H50	-2212.26	7637.45	6079.28	34

H52A	2062	8279.46	10991.49	42
H52B	2430.52	9279.24	11191.4	42
H52C	2233.5	8665.55	10253.77	42
H53A	99.84	7660.92	6569.26	42
H53B	-908.98	7114.12	5906.7	42
H53C	-325.56	6782.07	6693.08	42
H55	4856.14	4381.47	6859.84	24
H57	4188.43	4907.35	9031.67	32
H59	3246.84	2576.69	7340.28	23
H63	2119.99	2683.71	6026.7	24
H65	646.6	380.72	4390.73	24
H67	3448.01	1061.93	4913.47	24
H71	3402.26	3998.41	5440.45	23
H73	4412.29	3922.75	3478.78	23
H75	4924.54	2262.11	4930.4	23
H79	5909.92	3176.28	6602.21	24
H81	6966.77	1227.49	7351.71	28
H83	4127.87	1093.39	6444.97	27

Table S8. Atomic Occupancy for complex **1**.

Atom Occupancy	Atom Occupancy	Atom Occupancy			
F22A	0.686 (15)	F23A	0.686 (15)	F24A	0.686 (15)
F22B	0.314 (15)	F23B	0.314 (15)	F24B	0.314 (15)

Crystal structure determination of complex **1**

Crystal Data for C₈₅H₅₆BCuF₂₄N₂OP₂ ($M = 1713.60$ g/mol): triclinic, space group P-1 (no. 2), $a = 15.2633(5)$ Å, $b = 16.5133(5)$ Å, $c = 16.9715(5)$ Å, $\alpha = 102.705(2)^\circ$, $\beta = 108.539(2)^\circ$, $\gamma = 97.064(2)^\circ$, $V = 3869.3(2)$ Å³, $Z = 2$, $T = 100$ K, $\mu(\text{CuK}\alpha) = 1.734$ mm⁻¹, $D_{\text{calc}} = 1.471$ g/cm³, 69044 reflections measured ($5.61^\circ \leq 2\theta \leq 134.172^\circ$), 13622 unique ($R_{\text{int}} = 0.2218$, $R_{\text{sigma}} = 0.1289$) which were used in all calculations. The final R_1 was 0.1417 ($I > 2\sigma(I)$) and wR_2 was 0.2793 (all data).

S4 Determination of singlet oxygen yield using singlet oxygen probe

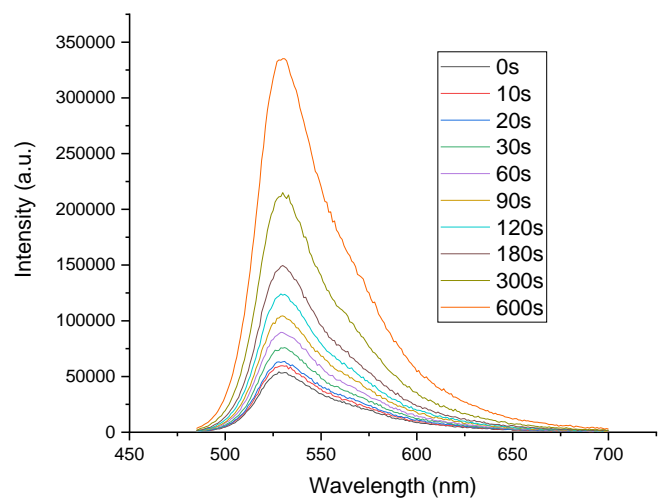
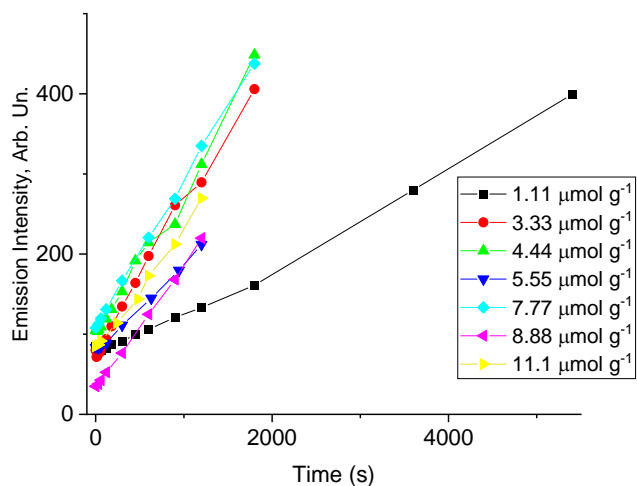


*Figure S9. Monitoring change in the emission spectrum of Singlet Oxygen Sensor Green in the presence of **1**-silica when irradiated with 10 mW cm^{-2} 405 nm light at varying time intervals. The intensity at 525 nm as a function of time is plotted in Figure 2 in the main text.*

a.



b.

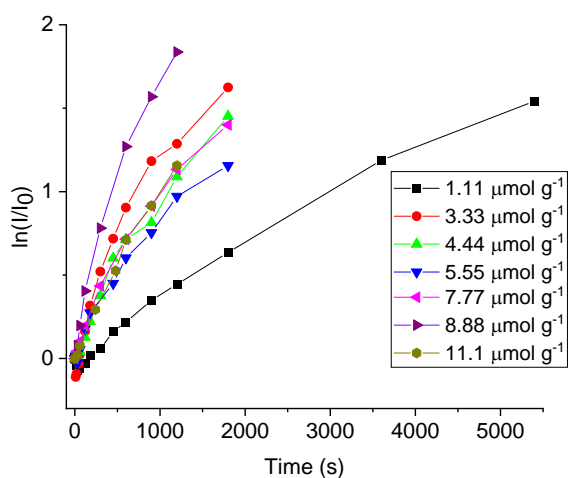


Figure S10. Monitoring change of a. emission intensity (I) at the emission maximum of Singlet Oxygen Sensor Green (525 nm), and b. $\ln(I/I_0)$ at SOSG emission maximum (525nm) as a function of time for different loading concentrations ($\mu\text{mol g}^{-1}$) of **1**-silica.

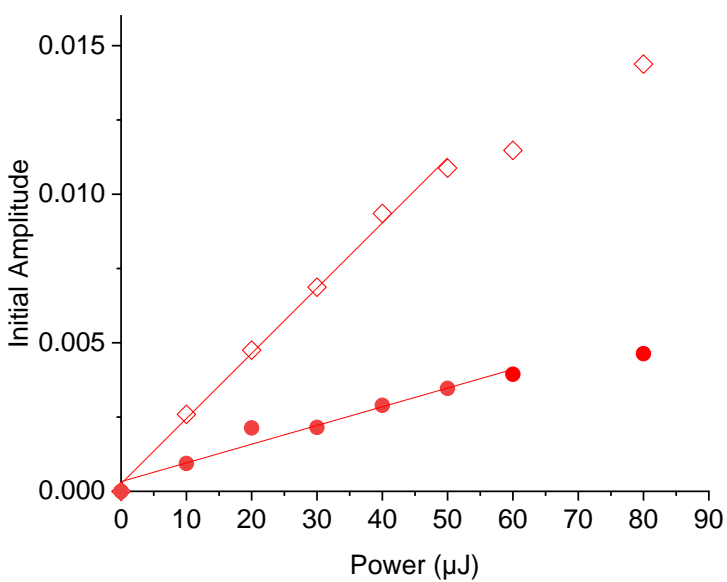


Figure S11. Direct measurement of singlet oxygen production in MeCN of complex **1** and perinapthenone (PN). The amplitude of singlet oxygen emission was measured at 1275 nm and extrapolated to zero time. The emission was measured as a function of laser excitation energy at 355 nm with an 8 ns pulse.

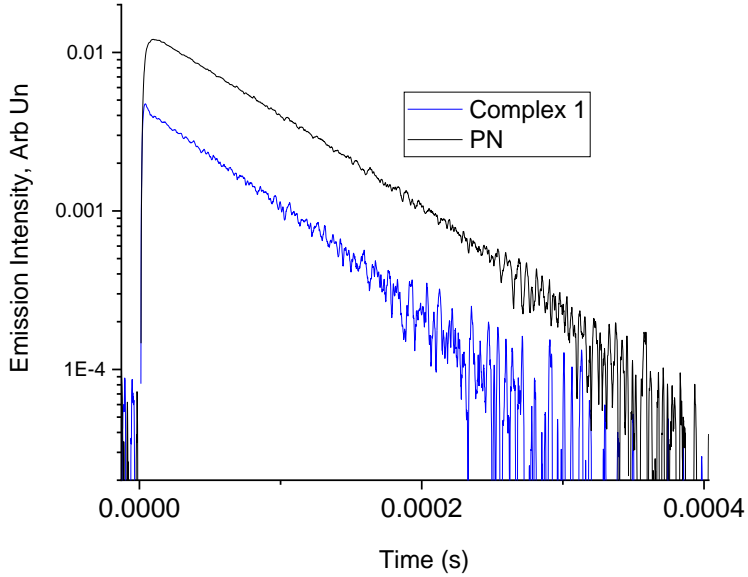


Figure S12. Decay trace of singlet oxygen emission at 1275nm (obtained by using a 355nm laser with 8ns pulse and a power of 80 μ J) in MeCN in the presence of Complex **1** and perinapthenone (PN). The figure illustrates that the lifetime of singlet oxygen is the same in both cases (72 μ s), therefore, no interaction between $^1\text{O}_2$ and complex **1** in its ground state is observed.

S5 Bacterial inactivation assay of MRSA in the presence of complex 1 in suspension

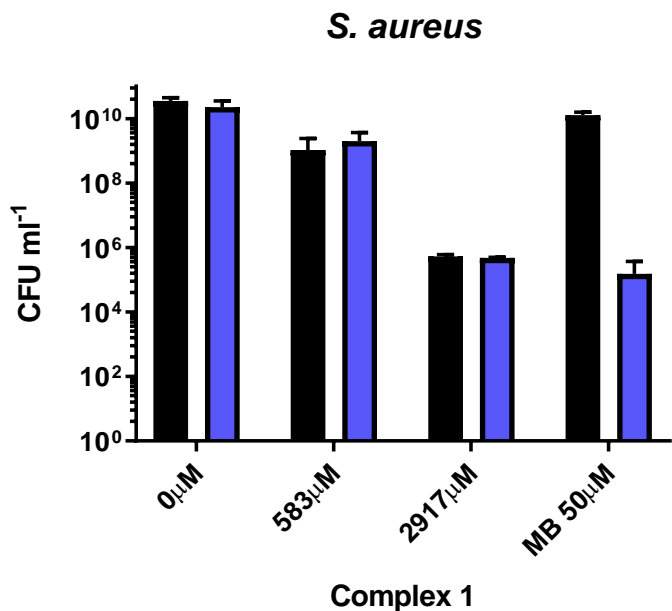
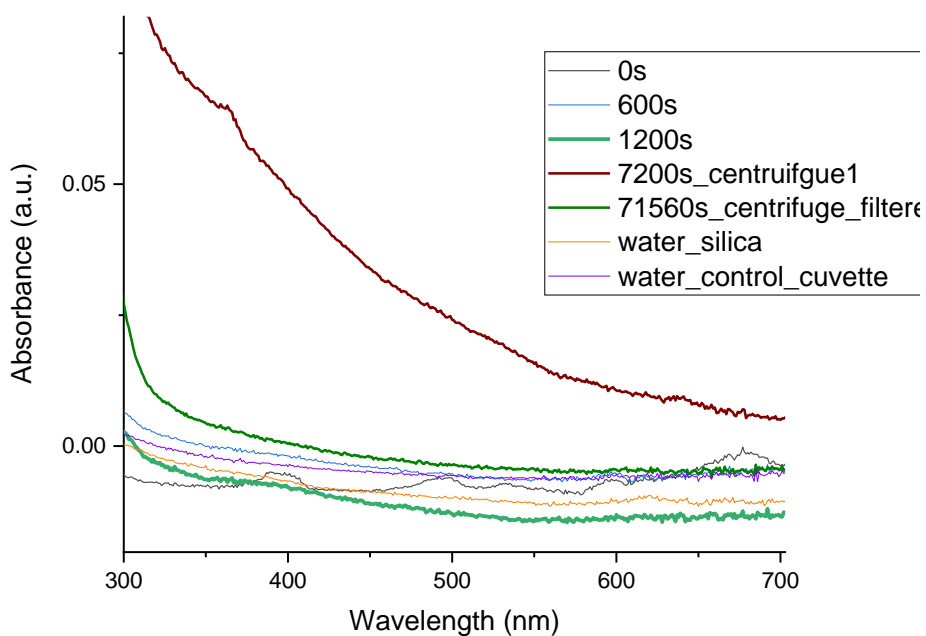


Figure S13. Bacterial viability assay measuring the colony forming units of *S. aureus* on its own ($0 \mu\text{M}$), in the presence of 1 mg ml^{-1} ($583 \mu\text{M}$) and 5 mg ml^{-1} ($2917 \mu\text{M}$) of complex 1, and methylene blue (MB) ($50 \mu\text{M}$). The samples were irradiated for 2 hours with 405 nm light at 17.5 mW cm^{-2} , total dose 126 J cm^{-2} (blue bars) or left in the dark for 2 hours (black bars).

S6 Stability of 1-silica

S6.1 Measuring the amount of leaching of complex 1 from silica through UV-Vis absorption of the suspension in water.

1-silica suspension (5 mg ml^{-1}) in water was stirred in a cuvette for 0s, 300s, 600s, 1200s, 1800s, 3600s and 7200s, figure S14. After being stirred a UV-Vis spectra of the solution was taken after letting the suspension settle in the cuvette. A final measurement was taken after 21 hours (71560s). In addition to settling the 7200s and 21 hour measurement were taken after using a centrifuge as the scatter from the silica remaining in suspension was too high. The supernatant of the 21 hour sample was also filtered due to high amounts of scatter. The lack of absorption spectra of **1** in the measurements taken suggests negligible solubility of the complex in solution. (The UV-Vis spectra are not normalised)



*Figure S14. UV-vis absorption spectra of **1**-silica suspension in water over time.*

S6.2 Measuring the amount of complex **1** before and after immobilisation on silica.

Uv-vis spectra of a solution of complex **1** in DCM (5 mg in 10ml) were recorded (Figure S15, **1_DCM_before**) before the complex (5mg) was dried onto silica (250 mg), equivalent to 10mg of complex **1** on 500mg of Silica as used in the antibacterial assays. After **1**-silica was removed, residual complex **1** remaining in the vessel was dissolved in 10ml of DCM and UV-vis measurement was taken (Figure S15, **1_DCM_residual**). **1**-Silica was the suspended in water and stirred for 2 hours. After 2 hours the solution was centrifuged and water was removed. 90mg of **1**-silica was recovered and complex **1** was removed using 3.6 ml of DCM (Figure S15, **1_DCM_after**). The difference in the before and after spectra is approximately equal to that of the residual measurement taken. This suggest that <0.3% of complex **1** was lost (by for example leaching) during the 2-hour experiment.

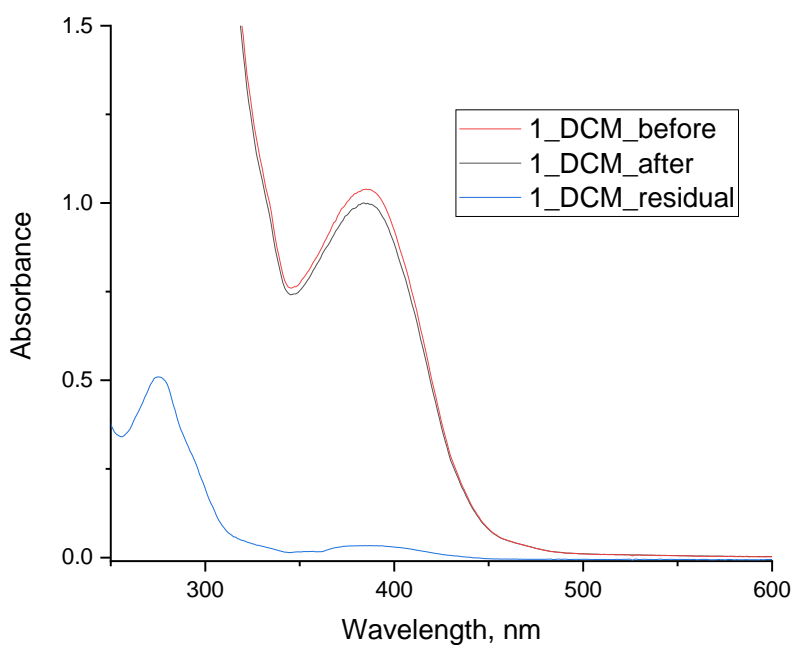


*Figure S15. UV-vis absorption spectra of complex **1** in DCM. Red line, solution (a): absorption spectrum of **1** prior to addition of silica (250 mg of silica in 10 ml of DCM, 5mg of complex **1**). Blue line, solution (b): The spectrum of the solution obtained by centrifuging silica, and filtering Black line (solution c): **1**-silica collected by centrifugation from solution “a” with silica added, stirred in water for 2 hrs, centrifuged, dried, and re-dissolved in DCM (90 mg of **1**-silica in 3.6 ml DCM, to match the originally taken 250 mg silica in 10 ml DCM).*

S7 Summary of relevant photosensitisers used for bacterial killing, as reported to date.

*Table S9. Summary of relevant photosensitisers used for bacterial killing, as reported to date. The examples superior to, or comparable with **1**-silica efficiency of bacterial killing are highlighted in green here and discussed in the main text of the paper.*

BODIPY - boron dipyrromethene, PAN - polyacrylonitrile nanofibers, A_3B^{3+} - 5-(4-aminophenyl)-10,15,20-tris-(4-N-methylpyridinium)porphyrin, Zn- A_3B^{3+} - [5-(4-aminophenyl)-10,15,20-tris-(4-N-methylpyridinium)porphyrinato]zinc(II), NFC - nanofibrillated cellulose, Zn(TMPyP) $^{4+}$ - zinc-tetra(4-N-methylpyridyl)porphine, PMB - polypeptide polymyxin B, TMPyP - 5,10,15,20-tetrakis(N-methylpyridinium-4-yl)porphyrin tetra-p-toluensulfonate, ZnPc - Zzinc(II) 2,9,16,23-tetrakis(N-methyl-pyridiumoxy)phthalocyanine tetraiodide, NOP - N-(3-aminopropyl)-3-(trifluoromethyl)-4-nitrobenzenamine, TPP - 5,10,15,20-tetraphenylporphyrin, TPPS - tetraphenylporphyrin sulfonate, trans-MePy $^+$ -NH $_2$ - trans-pyridinium aminoporphyrin, MB – Methylene Blue

Photo-sensitiser	Support	Wavelength	Irradiation time (min)	Power (mW cm $^{-2}$)	Fluence (J cm $^{-2}$)	Pathogen	Reduction	Amount/Concentration	Notes	Ref
Complex 1	Silica	405 nm	15	17.5	126	<i>S. aureus</i>	99.99%	55 μM		This work
	Silica	405 nm	120	17.5	126	<i>S. aureus</i>	99.9999%	55 μM		
	Silica	405 nm	120	17.5	189	<i>E. coli</i>	99.99%	55 μM	Induction period of 60 min observed	
	Silica	405 nm	180	17.5	189	<i>E. coli</i>	99.9999%	55 μM	Induction period of 60 min observed	
Re(CO) $_3$ derivatives	N/A	365 nm	60	0.83	3	<i>E. coli</i>	-	5.8 - 11.6 μM	Study of the minimum inhibitory concentration for each derivative.	12
[Ru(bpy-TMEDA) $_3$] $^{8+}$	N/A	470 nm	20	22	27	<i>S. aureus</i>	6.87log $_{10}$ reduction	15 μM	Initial concentration 10 8 CFU. In solution.	13
[Ir(phen) $_2$ (3,8-dipyrenyl-phen)] $^{3+}$	N/A	Visible light	~60	9.7	35	<i>S. aureus</i>	-	0.17 μM	*EC $_{50}$ measurement. In solution	14
[Ir(phen) $_2$ (3-pyrenyl-phen)] $^{3+}$	N/A	Visible light	~60	9.7	35	<i>S. aureus</i>	-	0.16 μM	*EC $_{50}$ measurement. In solution.	14
BODIPY	Nylon	400 – 700 nm	30	40	72	<i>S. aureus</i>	99.9999%	3.4 nmol mg $^{-1}$ of material	BODIPY photobleached after 30 min (118 J cm $^{-2}$). Thereafter 9 hr @65 mW cm $^{-2}$ is required to achieve similar level of killing	15
	Nylon	400 – 700 nm	60	65	234	<i>E. faecium</i> , <i>K. pneumoniae</i> , <i>A. baumannii</i>	99.9999%, 47%, 99.95%	3.4 nmol mg $^{-1}$ of material		15
	Nylon	400 – 700 nm	60	65	234	Vesicular stomatitis virus	Not stated	3.4 nmol mg $^{-1}$ of material	virus	15
	PAN	400 – 700 nm	30	40	72	<i>S. aureus</i>	99.9999%	35 nmol mg $^{-1}$ of material	BODIPY photobleached after 30 min (118 J cm $^{-2}$). Thereafter 11 hr @65 mW cm $^{-2}$ is required to achieve similar level of killing	15
	PAN	400 – 700 nm	60	65	234	<i>E. faecium</i> , <i>K. pneumoniae</i> , <i>A. baumannii</i>	99.9999%, 75%, 99.9999%	35 nmol mg $^{-1}$ of material		15
	PAN	400 – 700 nm	60	65	234	virus	99.99%	35 nmol mg $^{-1}$ of material	Vesicular stomatitis virus	15
A_3B^{3+}	NFC	400 – 700 nm	60	65	234	<i>S. aureus</i>	99.9999%	5 μM	99.9999% reduction at 0.5 μM of the sensitiser	16
	NFC	400 – 700 nm	60	65	234	<i>A. baumannii</i>	99.9938%	5 μM	99.9999% reduction at 20 μM of the sensitiser	16
	NFC	400 – 700 nm	60	65	234	<i>E. faecium</i>	99.9999%	5 μM		16
	NFC	400 – 700 nm	60	65	234	Dengue-1	99.9900%	5 μM	Virus	16
	NFC	400 – 700 nm	60	65	234	virus	99.9999%	5 μM	Vesicular stomatitis virus	16
	paper	400 – 700 nm	60	65	234	<i>S. aureus</i> , <i>A. baumannii</i> , <i>E. faecium</i>	99.9999%	5 μM		16
	paper	400 – 700 nm	60	65	234	<i>K. pneumoniae</i>	99.9994%	5 μM		16
Zn- A_3B^{3+}	NFC	400 – 700 nm	60	65	234	<i>S. aureus</i> , <i>A. baumannii</i> , <i>E. faecium</i>	99.9999%	5 μM		16
	NFC	400 – 700 nm	60	65	234	<i>K. pneumoniae</i>	66.0000%	5 μM		16

	NFC	400 – 700 nm	60	65	234	Dengue-1	99.990%	5 µM	Virus	16
	NFC	400 – 700 nm	60	65	234	virus	99.9999%	5 µM	Virus Vesicular stomatitis	16
	paper	400 – 700 nm	60	65	234	<i>S. aureus</i> , <i>A. baumannii</i> , <i>E. faecium</i>	99.9999%	5 µM		16
	paper	400 – 700 nm	60	65	234	<i>K. pneumoniae</i>	99.4700%	5 µM		16
Zn(TMPyP) ⁴⁺	Polyethylenelene-elastomer	400 – 700 nm	60	65	234	<i>S. aureus</i> , <i>E. faecium</i>	99.9999%	~10 mg g ⁻¹ of support	~1 cm diameter support	17
Zn(TMPyP) ⁴⁺	Polyethylenelene-elastomer	400 – 700 nm	60	80	288	<i>E. coli</i>	99.9500%	~10 mg g ⁻¹ of support	~1 cm diameter support	17
	Polyethylenelene-elastomer	400 – 700 nm	60	80	288	<i>A. baumannii</i>	99.8900%	~10 mg g ⁻¹ of support	~1 cm diameter support	17
	Polyethylenelene-elastomer	400 – 700 nm	60	80	288	<i>K. pneumoniae</i>	99.9600%	~10 mg g ⁻¹ of support	~1 cm diameter support	17
	Polyethylenelene-elastomer	400 – 700 nm	60	65	234	Had-5	99.9600%	~10 mg g ⁻¹ of support	Virus. ~1 cm diameter support	17
	Polyethylenelene-elastomer	400 – 700 nm	60	65	234	Vesicular stomatitis virus	99.9998%	~10 mg g ⁻¹ of support	Virus. ~1 cm diameter support	17
Chlorin-e6	Cellulose Nano-crystals w/ immobilised PMB	visible light	900	0.8	43.2	<i>S. aureus</i>	> 98.5%	0.191 mg ml ⁻¹	Reached detection limit, 300 CFU. PMB concentration 61.8 µg ml ⁻¹ .	18
		visible light	900	0.8	43.2	<i>E. coli</i>	> 98.5%	0.019 mg ml ⁻¹	Reached detection limit, 300 CFU. PMB concentration 6.2 µg ml ⁻¹	18
		visible light	900	0.8	43.2	<i>S. epidermidis</i>	> 98.5%	0.191 mg ml ⁻¹	Reached detection limit, 300 CFU. PMB concentration 61.8 µg ml ⁻¹ .	18
		visible light	900	0.8	43.2	<i>P. aeruginosa</i>	> 99.7%	0.019 mg ml ⁻¹	Reached detection limit, 300 CFU. PMB concentration 6.2 µg ml ⁻¹ .	18
TMPyP	Polystyrene with immobilised NOP	> 400 nm	10	500 W Xenon lamp	Not stated	<i>E. coli</i>	90%	5 cm ² (TMPyP 0.75 mmol g ⁻¹ or 0.68 mg cm ⁻² , NOP 1.65 mmol g ⁻¹ or 0.29 mg cm ⁻²)	Starting CFU 6000. Measurement on surface in an agar plate.	19
	Poly-styrene	> 400 nm	10		Not stated	<i>E. coli</i>	90%	5 cm ² (TMPyP 0.75 mmol g ⁻¹ or 0.68 mg cm ⁻² , NOP 1.65 mmol g ⁻¹ or 0.29 mg cm ⁻²)	Starting CFU 6000. Measurement on surface in an agar plate.	19
ZnPc	Polystyrene with immobilised NOP	> 400 nm	10	500 W Xenon lamp	Not stated.	<i>E. coli</i>	70%	5 cm ² (ZnPc: 0.46 mmol g ⁻¹ or 0.47 mg cm ⁻² , NOP: 1.65 mmol g ⁻¹ or 0.29 mg cm ⁻²)	Starting CFU 6000. Measurement on surface in an agar plate.	19
	Polystyrene	> 400 nm	10		Not stated	<i>E. coli</i>	70%	5 cm ² (ZnPc: 0.46 mmol g ⁻¹ or 0.47 mg cm ⁻² , NOP: 1.65 mmol g ⁻¹ or 0.29 mg cm ⁻²)	Starting CFU 6000. Measurement on surface in an agar plate.	19
TMPyP	Polystyrene with immobilised NOP	> 400 nm	10	500 W Xenon lamp	Not stated	<i>E. coli</i>	90%	5 cm ² . TMPyP: 0.75 mmol g ⁻¹ , 0.68 mg cm ⁻² , NOP: 1.65 mmol g ⁻¹ , 0.29 mg cm ⁻²	Starting CFU 6000. Measurement on surface in an agar plate.	19
	Polystyrene	> 400 nm	10		Not stated	<i>E. coli</i>	20%	5 cm ² . ZnPc: 0.46 mmol g ⁻¹ or 0.47 mg cm ⁻² , NOP: 1.65 mmol g ⁻¹ , 0.29 mg cm ⁻²	Starting CFU 6000. Measurement on surface in an agar plate.	19
ZnPc	Polystyrene with immobilised NOP	> 400 nm	10	500 W Xenon lamp	Not stated	<i>E. coli</i>	90%	5 cm ² (ZnPc: 0.46 mmol g ⁻¹ or 0.47 mg cm ⁻² , NOP: 1.65 mmol g ⁻¹ or 0.29 mg cm ⁻²)	Starting CFU 6000. Measurement on surface in an agar plate.	19
	Polystyrene	> 400 nm	10		Not stated	<i>E. coli</i>	15%	5 cm ² (ZnPc: 0.46 mmol g ⁻¹ or 0.47 mg cm ⁻²)	Starting CFU 6000. Measurement on surface in an agar plate.	19
TPP	Hydrophilic polycaproactone or polyurethane	White light	30	300 W Xenon lamp	Not stated	Polyoma-virus or baculovirus	Viral Inactivation	1 cm ² piece of support with 1% TPP	Viruses inactivated in the presence sensitiser-doped supports after 30 minutes of exposure to visible light	20
TPPS		White light	30	300 W Xenon lamp	Not stated	Polyoma-virus or baculovirus	Viral Inactivation	1 cm ² piece of support with 1% TPP	Viruses inactivated in the presence sensitiser-doped supports after 30 minutes of exposure to visible light	20
9,10-anthraquinone-2-carboxylic acid	Silica	> 340 nm (power given for 365 nm)	110	3.85	25.41	<i>E. coli</i>	~100%	700 µM	Initial CFU ~10 ⁶ reduced to undetectable level. Initial induction period of 60 min	21
TiO ₂	N/A	> 340 nm (power given for 365 nm)	90	3.85	20.79	<i>E. coli</i>	~100%	0.25 g L ⁻¹	Initial CFU ~10 ⁶ reduced to undetectable level. No induction period.	21
TPP	Poly-styrene	white light	60 - 90	150 W halogen bulb	Not stated	<i>E. coli</i>	Not stated	1% TPP	24 hrs post-irradiation, growth inhibition was observed	22
	Poly-urethane Larithane	white light	60 - 90	150 W halogen bulb	Not stated	<i>E. coli</i>	Not stated	1% TPP	24 hrs post-irradiation, growth inhibition was observed	22
	Poly-capro-lactone	white light	60 - 90	150 W halogen bulb	Not stated	<i>E. coli</i>	Not stated	1% TPP	24 hrs post-irradiation, growth inhibition was observed	22
	Poly-amide 6	white light	60 - 90	150 W halogen bulb	Not stated	<i>E. coli</i>	Not stated	1% TPP	24 hrs post-irradiation, growth inhibition was observed	22
TPP-NH ₂	Cellulose cotton	white light	24 hrs	0.001833	9.5	<i>S. aureus</i>	-	0.037 µmol mg ⁻¹ of support	Growth inhibition experiment. Neutral system.	23

TPPS-NH ₂	Cellulose cotton	white light	24 hrs	0.001833	9.5	<i>S. aureus</i>	-	0.03 µmol mg ⁻¹ of support	Growth inhibition experiment. Anionic system.	23
trans-MePy ⁺ -NH ₂	Cellulose cotton	white light	86400	0.001833	9.5	<i>S. aureus</i>	-	0.028 µmol mg ⁻¹ of support	Growth inhibition experiment. Cationic system.	23
ZnTPP	Poly-urethane	white light	30	150 W halogen bulb	Not stated	<i>E. coli</i>	No cell growth was observed	0.1% ZnTPP	Samples were irradiated for 30 min and left to incubate for 24 hrs.	24
ZnPc	Poly-urethane	white light	30	150 W halogen bulb	Not stated	<i>E. coli</i>	No cell growth was observed	0.1% ZnPc	Samples were irradiated for 30 min and left to incubate for 24 hrs.	24
TPP	Poly-urethane	white light	60	150 W halogen bulb	Not stated	<i>E. coli</i>	No cell growth was observed	0.12% TPP	Polyurethane, doped w/0.6% sodium dodecyl sulfate	25
[(4,7-Ph ₂ -1,10-phen) ₃ Ru] ²⁺ (RDP2)	Porous Si in a solar reactor	> 373 nm	540	200	Not stated	<i>E. coli</i>	1.1 x 10 ⁵ CFU hr ⁻¹ L ⁻¹	1-30 mg g ⁻¹	Water flowed through reactor at 15 ml hr ⁻¹ . Disinfection rate of 1.1 x 10 ⁵ CFU hr ⁻¹ L ⁻¹	26
MB	-	sunlight	30	74.3	133.74	<i>E. coli</i>	99.5%	10 mg L ⁻¹	In solution	27
	Poly-styrene	white light	60	4 TLE 22 W23, Phillips lamps	Not stated	<i>E. coli</i>	97.3%	20 g L ⁻¹	Surface loading not stated	28
	Silica	white light	60		Not stated	<i>E. coli</i>	65%	20 g L ⁻¹ (0.5 mg g ⁻¹ of silica)	-	28
	XAD-2 resin	white light	60		Not stated	<i>E. coli</i>	75.6%	20 g L ⁻¹ (0.2 mg g ⁻¹ of silica)	-	28
	Granular activated carbon	white light	60		Not stated	<i>E. coli</i>	94.8%	20 g L ⁻¹ (2 mg g ⁻¹ of silica)	-	28

References

- 1 C. S. Smith, C. W. Branham, B. J. Marquardt and K. R. Mann, *Journal of the American Chemical Society*, 2010, **132**, 14079–14085.
- 2 Y. Zhang, P. Traber, L. Zedler, S. Kupfer, S. Gräfe, M. Schulz, W. Frey, M. Karnahl and B. Dietzek, *Physical Chemistry Chemical Physics*, 2018, **20**, 24843–24857.
- 3 M. Heberle, S. Tschierlei, N. Rockstroh, M. Ringenberg, W. Frey, H. Junge, M. Beller, S. Lochbrunner and M. Karnahl, *Chemistry - A European Journal*, 2017, **23**, 312–319.
- 4 R. Giereth, I. Reim, W. Frey, H. Junge, S. Tschierlei and M. Karnahl, *Sustainable Energy and Fuels*, 2019, **3**, 692–700.
- 5 Y. Zhang, M. Heberle, M. Wächtler, M. Karnahl and B. Dietzek, *RSC Advances*, 2016, **6**, 105801–105805.
- 6 D. García-Fresnadillo, Y. Georgiadou, G. Orellana, A. M. Braun and E. Oliveros, *Helvetica Chimica Acta*, 1996, **79**, 1222–1238.
- 7 Bruker, 2016.
- 8 L. Krause, R. Herbst-Irmer, G. M. Sheldrick and D. Stalke, *Journal of Applied Crystallography*, 2015, **48**, 3–10.
- 9 G. M. Sheldrick, *Acta Crystallographica Section A: Foundations of Crystallography*, 2015, **71**, 3–8.
- 10 G. M. Sheldrick, *Acta Crystallographica Section C: Structural Chemistry*, 2015, **71**, 3–8.
- 11 O. V. Dolomanov, L. J. Bourhis, R. J. Gildea, J. A. K. Howard and H. Puschmann, *Journal of Applied Crystallography*, 2009, **42**, 339–341.

- 12 A. Frei, M. Amado, M. A. Cooper and M. A. T. Blaskovich, *Chemistry - A European Journal*, 2020, **26**, 2852–2858.
- 13 Y. Feng, W. Z. Sun, X. S. Wang and Q. X. Zhou, *Chemistry - A European Journal*, 2019, **25**, 13879–13884.
- 14 L. Wang, S. Monro, P. Cui, H. Yin, B. Liu, C. G. Cameron, W. Xu, M. Hetu, A. Fuller, S. Kilina, S. A. McFarland and W. Sun, *ACS Applied Materials and Interfaces*, 2019, **11**, 3629–3644.
- 15 K. R. Stoll, F. Scholle, J. Zhu, X. Zhang and R. A. Ghiladi, *Photochemical and Photobiological Sciences*, 2019, **18**, 1923–1932.
- 16 D. R. Alvarado, D. S. Argyropoulos, F. Scholle, B. S. T. Peddinti and R. A. Ghiladi, *Green Chemistry*, 2019, **21**, 3424–3435.
- 17 B. S. T. Peddinti, F. Scholle, R. A. Ghiladi and R. J. Spontak, *ACS Applied Materials and Interfaces*, 2018, **10**, 25955–25959.
- 18 F. le Guern, T. S. Ouk, K. Grenier, N. Joly, V. Lequart and V. Sol, *Journal of Materials Chemistry B*, 2017, **5**, 6953–6962.
- 19 J. Dolanský, P. Henke, P. Kubát, A. Fraix, S. Sortino and J. Mosinger, *ACS Applied Materials and Interfaces*, 2015, **7**, 22980–22989.
- 20 Y. Lhotáková, L. Plíštil, A. Morávková, P. Kubát, K. Lang, J. Forstová and J. Mosinger, *PloS one*, 2012, **7**, e49226.
- 21 A. K. Benabbou, C. Guillard, S. Pigeot-Rémy, C. Cantau, T. Pigot, P. Lejeune, Z. Derriche and S. Lacombe, *Journal of Photochemistry and Photobiology A: Chemistry*, 2011, **219**, 101–108.
- 22 S. Jesenská, L. Plíštil, P. Kubát, K. Lang, L. Brožová, Š. Popelka, L. Szatmáry and J. Mosinger, *Journal of Biomedical Materials Research - Part A*, 2011, **99 A**, 676–683.
- 23 C. Ringot, V. Sol, M. Barrière, N. Saad, P. Bressollier, R. Granet, P. Couleaud, C. Frochot and P. Krausz, *Biomacromolecules*, 2011, **12**, 1716–1723.
- 24 J. Mosinger, K. Lang, P. Kubát, J. Sýkora, M. Hof, L. Plíštil and B. Mosinger, *Journal of Fluorescence*, 2009, **19**, 705–713.
- 25 J. Mosinger, O. Jirsák, P. Kubát, K. Lang and B. Mosinger, *Journal of Materials Chemistry*, 2007, **17**, 164–166.
- 26 M. E. Jiménez-Hernández, F. Manjón, D. García-Fresnadillo and G. Orellana, *Solar Energy*, 2006, **80**, 1382–1387.
- 27 A. T. Cooper and D. Y. Goswami, *Journal of Solar Energy Engineering, Transactions of the ASME*, 2002, **124**, 305–310.
- 28 A. Savino and G. Angeli, *Water Research*, 1985, **19**, 1465–1469.